→ ESA DIVERSITY II - DRYLAND PRODUCTS

Booklet for Test Site 06 | Central Tibetan Plateau

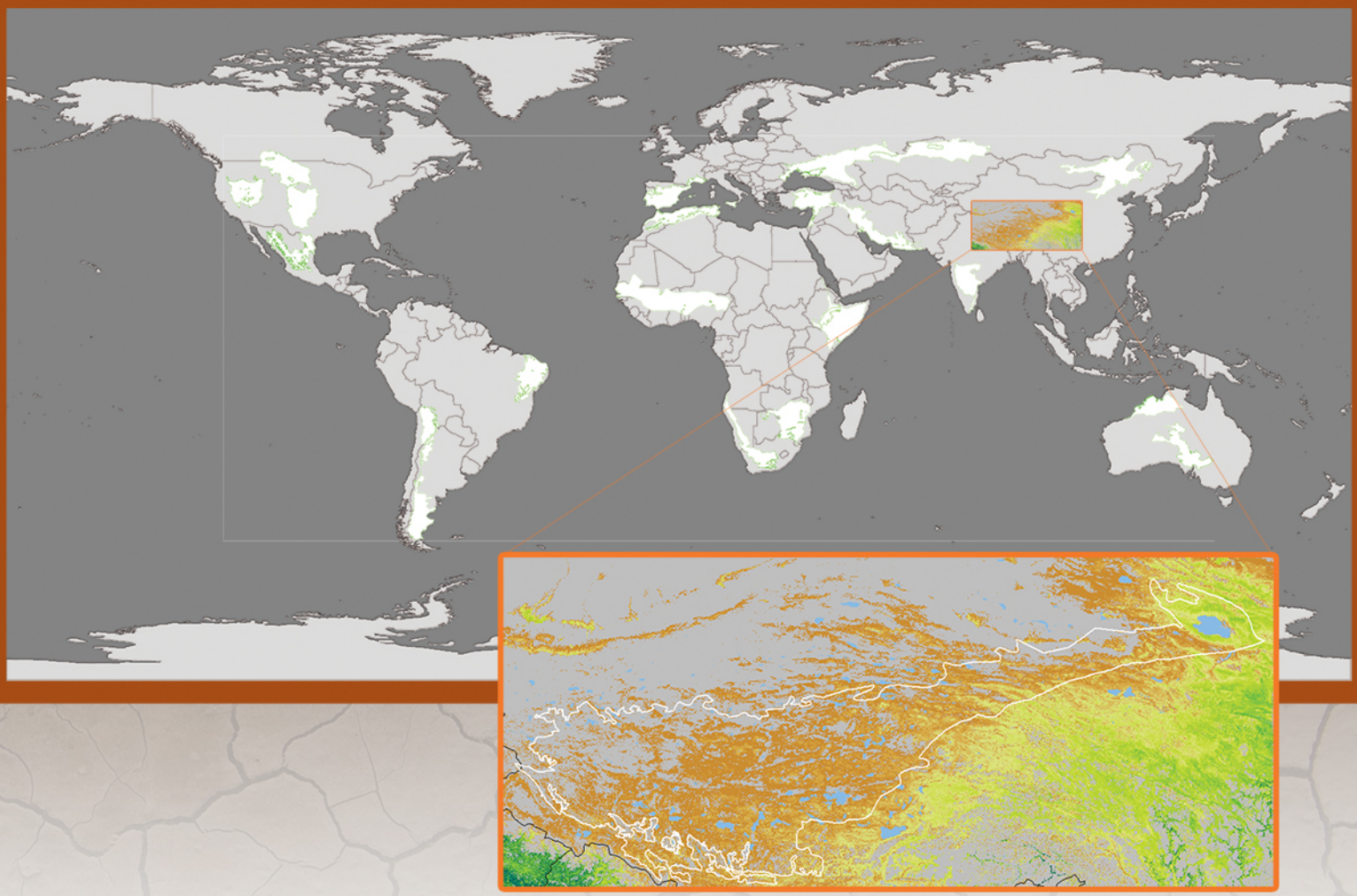

European Space Agency

All Drylands Booklets are available on **www.diversity2.info**

Publisher	ESA Diversity II project
Editor	Ute Gangkofner (GeoVille, Austria)
Cover Design	ESA - EOGB (Earth Observation Graphic Bureau)

Acknowledgement

This booklet as one of 22 in total presents dryland results of the ESA DUE DiversityII project, where we thank ESA for the project initiative and funding. The providers of the global meteorological and biophysical data sets are acknowledged and thanked for making the data available free of charge: the University of Maryland; Department of Geography for the NOAA GIMMS NDVI data, NASA for the TRMM rainfall data, NOAA for the GPCP precipitation data, and the TU Vienna for the CCI soil moisture data. We are grateful to users and addressees for their feedback, valuable information, and their contributions to the user meetings. The project results and their presentation in the booklets owe their existence to many persons, whose affiliations are presented on the back cover of the booklet. A special thank is owed to Bob Scholes and Graham v. Maltitz, who kindly contributed "desertification narratives" about site 12, Southern Africa West, and respectively site 21, Southern Africa East.

About the Booklet

The booklets provide information about the vegetation condition of major dry regions of the world and how it developed during the first decade of this century as seen by ENVISAT MERIS. Focus is on vegetation productivity combined with detailed phenological analyses. The booklets present part of the developed indicators, which comprise status and trend/change information.

Chapter 1 gives a short introduction to the Diversity II project and the scope of the booklet.

Chapter 2 introduces the test site with a condensed biodiversity summary, and a regional "dryland" story, which users might relate to some of the map products provided. Further overview information is given such as LCC Land Cover and aridity maps, as well as climate diagrams.

Chapter 3 is a short overview of the data and methods applied.

Chapter 4 describes the developed indicators and presents selected indicator maps.

Chapter 5 discusses the indicators and their information content.

Chapter 6 contains a short outlook.

Annex 1 contains more detailed biodiversity descriptions for five dryland test sites: site 10 Southern Europe, site 12 Southern Africa West, Site 13 Western Sahel, site 15 Caatinga, Brazil, and site 20 Southern Australia.

Table of Contents

Figures

Tables

1 Introduction to Diversity II

With the Diversity II project ESA aims at contributing with EO based methods to the strategic goals of the Convention on Biological Diversity (CBD), especially the supportive goal E: Enhance implementation through participatory planning, knowledge management and capacity building. Besides the CBD and other interested parties, also the UN Convention to Combat Desertification (UNCCD) is a major relevant and interested stakeholder. **The specific aim of this project is to set up an EO-based monitoring scheme for the assessment of status, changes and trends of biodiversity and ecosystem NPP (Net Primary Production) in global drylands using moderate resolution EO data.** The project is primarily based on ENVISAT MERIS data, which have been recorded from June 2002 to April 2012. Figure 1 gives an overview of the selected dryland sites, which constitute WWF (World Wildlife Fund) ecoregions.

Figure 1: Distribution of global Diversity II dryland sites with internal numbering

1.1 Scope of the Booklet

The booklet compiles and summarizes important outcomes per test site, and thus constitutes a regional complement to the project reports and the product user handbook (PUH). The PUH provides in depth and complete project documentation, though without highlighting every test site.

Interested users, for instance those who will not look at the map files themselves, will find some major results presented in the booklet, as well as a short description of the methodology and of the individual products shown.

The booklets and the PUH can be downloaded at http://www.diversity2.info/products/.

2 The Test Site *Central Tibetan Plateau*

Dryland Story of Central Tibetan Plateau

The fragile environment, warming over the past 50 years and the partially heavy droughts combined with over-population and the heavy exploitation of natural resources lead to ongoing desertification processes in the Central Tibetan Plateau. Figure 2 shows the area (ha) of degraded land in different parts of the Tibetan Plateau according to Xue-Yong et al. 2002.

There is a controversy about the causes of desertification on the Tibetan Plateau

"Sanjiangyuan – which literally translates as the 'three river source area' – feeds China's mightiest rivers. The 300,000-square kilometre region, high on western China's Qinghai-Tibetan plateau, provides a quarter of the Yangtze's water, almost half of the Yellow River's and 10% of the Mekong's. Crucial as this area is, its environment is deteriorating, with rising snowlines, shrinking lakes, wetland degradation and reduced runoff. As early as 2001, over 90% of Qumarleb county's wells were found to be empty, while 100 of Madoi county's 4077 lakes had dried up. More than half of the usable grassland is severely degraded, suffering desertification or over-run with pests.The situation has been compounded by a sharp drop in biodiversity, both in absolute numbers and types of species. More than 100,000 Tibetan antelope – a "grade one" state protected species – used to roam the plateau. Numbers fell to just 30,000 at their ebb, though recently the population has been rising again. The alpine musk deer is on the brink of extinction, and there has been a sharp drop in the numbers of white lipped deer, red deer and snow leopards".

Source: https://www.chinadialogue.net/article/show/single/en/5621-Climate-change-not-grazing-destroying-the-Tibetan-Plateau. According to this source, it is predominantly climate change that leads to this accelerated desertification.

Figure 2: „Tibet's disappearing grasslands", Source:

https://www.chinadialogue.net/article/show/single/en/3828-Tibet-s-disappearing-grasslands

"*Scientists say the desertification of the mountain grasslands is accelerating climate change. Without its thatch, the roof of the world is less able to absorb moisture and more likely to radiate heat*".

Areas	Desertification land in different classes										
	Severely desertified land	Moderately desertified land		Slightly desertified land		Severe salinized land		Subtotal of desertified land	Potentially desertified land	Total	Percentage of desertified land (%)
	Mobile sand land	Semi-stabilized sand land	Denuded gravel land	Stabilized sand land	Semi-bare gravel land	Saline desert	Sandy saline-alkali land				
Nagqu	100,790·85	576,332·65	5,933,383·09	74,615·92	3,341,895·41	961·41	241,632·11	10,269,611·44	1,049,895·26	11,319,506·70	51·83
Ali	45,989·04	47,592·79	2,726,454·94	—	3,230,632·25	508·58	238,391·48	6,289,569·08	133,249·94	6,422,819·02	29·41
Xigaze	140,082·38	277,428·05	1,492,197·66	146,412·62	1,258,945·12	—	12,919·54	3,327,985·37	91,562·80	341,9548·17	15·66
Shannan	35392·91	21,508·68	39,583·60	22,869·34	56,618·51	—	4,360·17	180,333·21	23,185·76	203,518·97	0·93
Qamdo	—	2,686·14	1,153·64	2,048·52	144,396·23	—	—	150,284·53	47,857·39	198,141·92	0·91
Lhasa	8,642·06	33,151·20	17,143·18	36,628·72	74,009·46	—	813·11	170,387·73	15,223·21	185,610·94	0·85
Nyingchi	5,566·80	9473·83	537·71	10251·73	59931·41	124·03	57·53	85943·04	4206·13	90149·17	0·41
Total	336,464·04	968,173·34	10,210,453·82	292,826·85	8,166,428·39	1,594·02	498,173·94	2,047,411·40	1,365,180·49	21,839,294·89	100·00

Table 1: Area (ha) of desertified land in different parts of the Tibetan Plateau.

As also featured above, one of the biggest problems in the area is the rangeland degradation in the Qinghai-Tibetan Plateau. Further on, according to a statistic of Harris et al. (2010) 90% of China's grasslands are degraded and the process of degradation is increasing at a rate of 200km²/yr. Besides climate change, the over-stocking with cattle, unsustainable livestock management, and specific agricultural practices contribute to these developments (Harris 2010).

References

Harris, R.B. (2010), Rangeland degradation on the Qinghai-Tibetan plateau: A review of the evidence of its magnitude and causes. Journal of Arid Environments, 74, 1–12.

Xue-Yong, Z., Sen, L., Chun-Lai, Z., Guang-Rong, D., Yu-Ziang, D. and Ping, Y. (2002), Desertification and control plan in the Tibet Autonomous Region of China. Journal of Arid Environments, 51, 183-198.

Additional References

Du, M., Yonemura, S., Thang, X., He, Y., Liu, J. and Kawashima, S. (2012), Climatic Warming due to Overgrazing on the Tibetan Plateau. Journal of Arid Land Studies, 22, 119-122.

Wang, X.D., Zhong, X.H., Liu, S.Z., Wang, Z.Y. and Li, M.H. (2008), Regional assessment of environmental vulnerability in the Tibetan Plateau: Development and application of a new method. Journal of Arid Environments, 72, 1929-1939.

Yang, M., Wang, S., Yao, T., Gou, X., Lu, A. and Guo, X. (2004), Desertification and its relationship with permafrost degradation in Qinghai-Xizang (Tibet) plateau. Cold Regions Science and Technology 39, 47–53.

2.1 Overview of Land Cover and Climate of the Test Site

The study AOI is the WWF ecoregion Central Tibetan Plateau alpine steppe (PA1002, https://www.worldwildlife.org/ecoregions/pa1002).

For most of the ecoregions, information on geography, biodiversity, threads, etc. is found on http://www.eoearth.org/view/article/51cbed7a7896bb431f692731/?topic=51cbfc77f702fc2ba8129ab9. Inserting the ID of the ecoregion or the name into the search window will lead to the respective ecoregion description site.

The maps in Figure 3 provide an overview of the study site. The upper map presents the CCI Land Cover v1.4 2010 data, which were derived (http://www.esa-landcover-cci.org/) based on ENVISAT MERIS (300m) data. Below, the CGIAR-CSI global aridity index map (Zomer et al. 2007, Zomer et al. 2008) is shown. The CGIAR-CSI global aridity index is computed as ratio of mean annual precipitation and mean annual potential evapotranspiration. Note that declining values indicate increasing aridity.

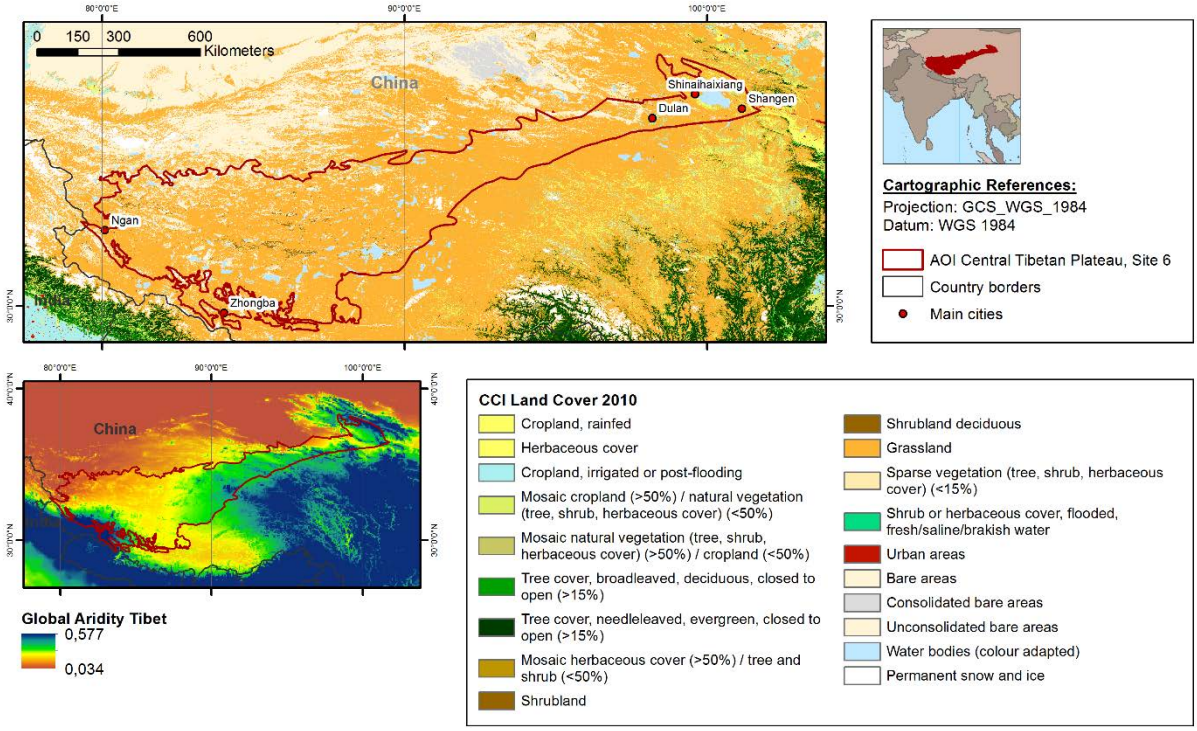

Figure 3: Overview of test site 06, Central Tibetan Plateau, showing land cover from the CCI Land Cover data set on the left-hand side and an aridity index map on the right-hand side derived from the CGIAR-CSI global aridity data base.

While the larger test site within the rectangle spans a broad spectrum of climatic conditions ranging from hyper-arid to humid, the actual AOI contains mainly semi-arid land. The overall land cover patterns reflect roughly the aridity gradients, and range from sparse vegetation to croplands and forests.

Figure 4 shows a climograph of Lhasa, Tibet, which exhibits distinct precipitation and temperature maxima in the summer months.

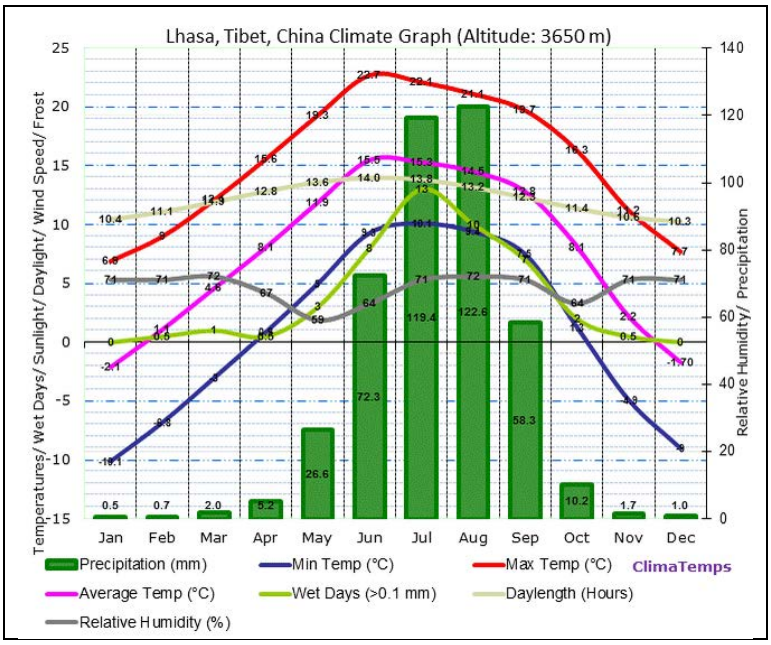

Figure 4: Climograph of Lhasa, Tibet. Source: http://www.tibet.climatemps.com/

2.2 Biodiversity Highlights in the Study AOI

Despite the serious ongoing desertification, the Tibetan Plateau is counted to the most pristine areas worldwide. The alpine steppes of the Central Tibetan Plateau located at elevations of 5000m or higher are mostly covered by small grasses and cushion plants, which sustain herds of ungulates like Tibetan antelope (*Pantholops hodgsoni*), Tibetan gazelles (*Procapra picticaudata*) and Tibetan wild asses (*Equus hemionus*). Important carnivores are also present such as lynx (*Felis lynx*), wolves (*Canis lupus*), snow leopards (*Panthera uncia*), and brown bears (*Ursus arctos*).

3 Materials and Methods

Based on ENVISAT MERIS FR and RR (Full and Reduced Resolution) data with a spatial resolution of 300m and respectively 1200m, all NPP proxies presented here and the indicators derived therefrom originate from the fraction of absorbed photosynthetically active radiation (fAPAR) computed according to Gobron et al. 2011. The fAPAR values are compiled on a bi-weekly basis, resulting in time series data with 24 halfmonthly values per calendar year. In addition, TRMM 3b42 rainfall data (http://trmm.gsfc.nasa.gov/) were used to relate the productivity data to precipitation, as well as CCI soil moisture data (http://www.esa-soilmoisture-cci.org/) as alternative data for water availability. Beyond 50° North and South, GPCP (http://www.gewex.org/gpcpdata.htm) rainfall data were taken, as TRMM data end at 50° N and S. For the period prior to the MERIS period, NOAA GIMMS NDVI data (http://glcf.umd.edu/data/gimms/) and GPCP rainfall data were confronted to show the "historical" development of vegetation and rainfall from 1982 to 2002 (map P56), i.e. prior to the MERIS period.

3.1 Generation of NPP-Proxies

In a first step, phenological parameters are derived individually for each year and pixel, shown in Figure 5. The diagram shows the temporal course of the MERIS fAPAR data during a 3-year period and the subdivision into different seasonal periods. The ***vegetation year*** includes the full yearly vegetation cycle starting at the turning of the preceding *dry or cold season* to the green season and ending after the following ***dry/cold season*** – or in case of several green seasons during a year – at the begin of the (statistically) dominant green season. The ***vegetation year length*** varies with

possible shifts of the green season start time, which results from the high rainfall variability typical for drylands. The average (median) start time of the vegetation years starting in 2003 to 2010 is presented in map P57.

The ***vegetation year*** can be subdivided into different periods, limited by defined starting and ending points in time. The ***growing season*** includes the major peak(s), i.e. ascending and descending parts of the time series and starts once a selected greenness threshold is surpassed on the way from the SoS to the green peak. The starting time of the growing season is shown in map P59. The ***dry season*** (brown parts of the curve) starts once a defined lower fAPAR threshold is passed. The thresholds depend on the seasonal amplitude and especially on the average level of the dry season values.

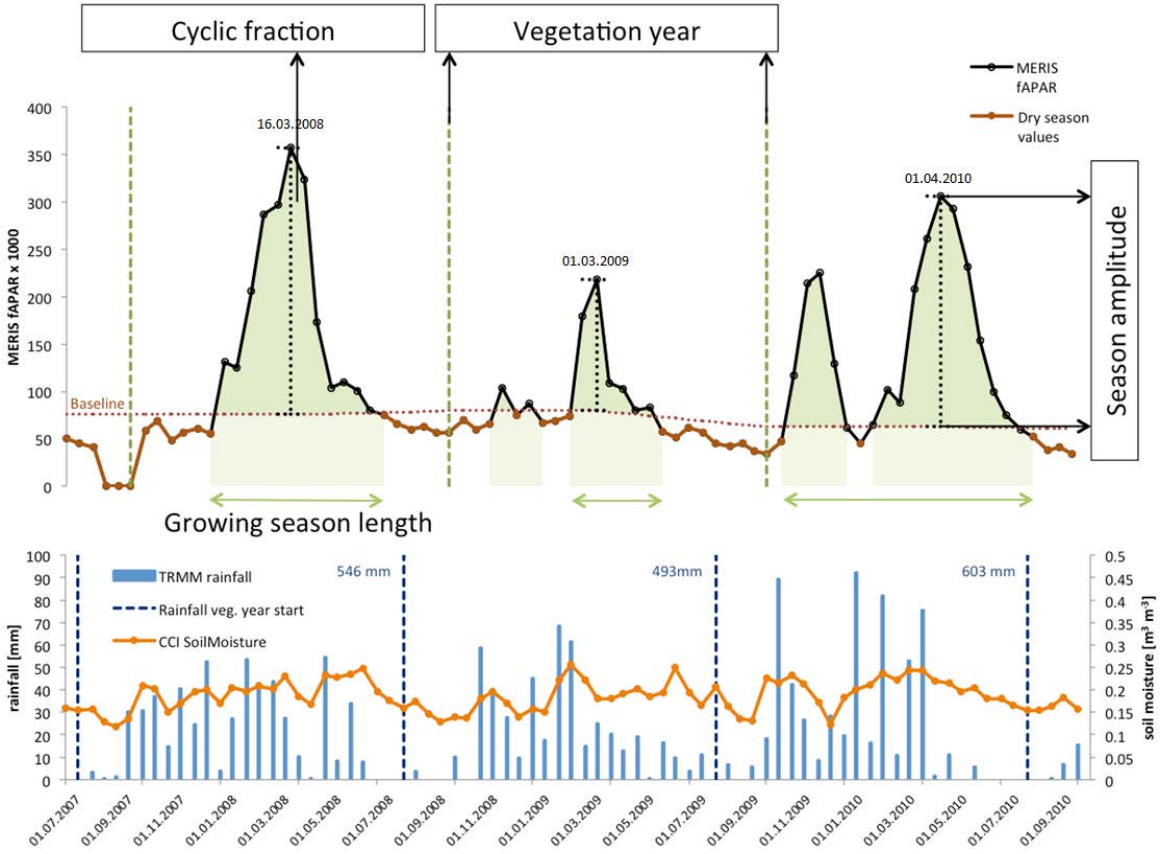

Figure 5: Scheme of the extracted phenological parameters, and corresponding rainfall and soil moisture data. (Location: South Africa, X: 25.7373764, Y: -29.896337)

The growing season length is shown in map P58. For the above described phenological periods, the MERIS fAPAR values have been temporally integrated to either sum or average values. The results are called "***NPP proxies***", and constitute yearly (one value per vegetation year) values. The developed indicator maps are primarily based on the following NPP proxies:

- ***Average vegetation year fAPAR:*** Mean value of all fAPAR values within one full vegetation cycle, constituting a proxy for the annual NPP (map P01) and/or standing green biomass.

- ***Cyclic fraction fAPAR:*** The cyclic fraction of the vegetation is comprised of summed fAPAR values of the green peak(s) during a vegetation year, subtracting the non-cyclic base levels. The cyclic fraction fAPAR can be interpreted as the amount of NPP that is directly related to the annual cycle of the climatic vegetation growth factors, especially rainfall (map P02).

- ***Average dry season fAPAR:*** For the dry season the low fAPAR values after the green peak are averaged. The dry season greenness values reflect the portion of plants that remain green after senescence of the annual vegetation or grow new green leaves during the dry period. High dry season levels indicate the presence of shrubs, bushes and trees (map P03).

- ***Percent cyclic vegetation of vegetation year greenness:*** The share of the cyclic vegetation of the entire vegetation year NPP is expected to decline with the increasing presence of evergreen vegetation. Shrublands and forests (with fully or partly green leaves in the dry period) thus tend to have lower values for this indicator than crops and grassland (this indicator is contained in two second order indicators, see map P50 and P51).

Rain Use Efficiency and Soil Moisture Use Efficiency

In addition to the NPP proxies, Rain Use Efficiency (RUE) and Soil Moisture Use Efficiency (SMUE) indicators were derived, in order to relate vegetation productivity and its spatial patterns and temporal variability to rainfall. While RUE is based on a widely applied, tested, discussed, and partly modified approach of Le Houérou (1984), SMUE is an analogue concept based on soil moisture data instead of rainfall as water availability parameter. Le Houérou defined RUE as *quotient of annual primary production by annual rainfall*. RUE thus expresses the amount of biomass growing per unit rainfall water. Theoretically, soil moisture is more directly related to plant water availability than rainfall, so SMUE is offered as a potentially useful additional indicator. RUE (and assumedly also SMUE) depends heavily on climate, soil properties, and vegetation conditions. For instance, as Le Houérou states, it decreases with increasing aridity due to the decreasing rate of useful rainwater (increasing evaporation, heavy rains, soil crusting and consequently more runoff, etc.).

It further depends on the way it is derived, especially the input parameters/data sources used for vegetation and rainfall. Since RUE is known to not necessarily normalize vegetation productivity based on rainfall variability, as RUE can be found to be correlated with rainfall over the years at a given place, its actual usefulness as an indicator for vegetation degradation (where RUE is supposed to decrease) is therefore limited and widely disputed. Nevertheless, we have included RUE and SMUE status and trend products in our products and the users may decide about its usefulness. Respective RUE and SMUE trend products are shown in the maps P37 and P40.

The function of RUE (or SMUE) as status indicator of ecosystem productivity and its usefulness for the comparison of the productivity of different ecosystems as proposed by Le Houérou (1984) is obvious and demonstrated in the maps P08, P17.

4 Generated Indicators

4.1 From NPP Proxies to First Order Indicators

By analyzing the annual NPP proxies and RUE/SMUE indicators and rainfall and soil moisture through time, a set of indicators for vegetation/ecosystem condition and change was derived. These can be divided into status and trend type indicators. Given the MERIS data period from June 2002 to April 2012 and the globally varying vegetation cycles, NPP proxy and RUE/SMUE indicators for a total of eight vegetation years could be extracted, starting in 2003/(2002) and ending in 2011/(2012).

Hence, MERIS based status and trend indicators cover worldwide eight vegetation years. Status indicators for this period include 8-year averages (maps P02, P03) and the coefficients of variation (maps P04, P26, P30P30). In addition, the 8-year period was subdivided into two epochs covering four vegetation years each. Epochal status maps and difference maps were generated for rainfall and soil moisture. The epochal difference map for rainfall is shown for rainfall in this booklet (map P46).

The trend slope maps were derived with the non parametric Theil Sen trend slope estimator (Theil 1950, Sen 1968) and constrained with the Mann Kendall significance test (Kendall 1962) to trends with a probability greater than 0.9 (maps P37 P40P40).

All indicator maps have been classified into distinct ranges of the original continuous values, using the same class intervals and colour scheme worldwide. For this reason the maps are globally comparable, though in rare cases not locally optimized. However, users can apply their own colour schemes to their individual downloaded maps, and in addition to the classified maps, also **the underlying continuous data sets are provided for further analyses on request**.

4.2 From First Order to Second Order Indicators

The first order status and trend indicators have been combined to derive more abstract and synoptic, second order indicators showing status, changes and trends of the most essential first order indicators in various relations to each other. Basically three types of such combinations were generated:

1. Relation between NPP proxies (vegetation year average greenness) and the percent of cyclic vegetation of vegetation year greenness

This indicator group highlights status, changes and trends of the relation between the two first order indicators. The status indicator (map P50) can be regarded as a functional classification of vegetation productivity and basic type: perennial versus annual/seasonal/ephemeral vegetation. The respective map is closely related to land use/cover patterns and also to soil type and terrain structures. The change indicator (map P51) displays epochal (2003-2006 versus 2007-2010) changes between the aggregated classes of the two underlying first order indicators.

2. Trend relation between vegetation year greenness and seasonal greenness

This indicator combines the vegetation year greenness trends with those of the cyclic vegetation and the dry season greenness. It has commonalities with P51, but the trend patterns deviate partly from the change patterns. Essentially this indicator (map P52) shows the development of the perennial and seasonal green vegetation in relation to each other during the observation period. For example, a positive vegetation year or dry season trend without a positive cyclic vegetation trend may possibly exhibit the dominant growth of bushes/trees versus cyclic vegetation. Vice versa, a prevailing positive trend of the cyclic vegetation may potentially point to a dominant increase of crop areas or grasses.

3. Direct relation between Rainfall and Vegetation Productivity

As an alternative to RUE/SMUE trends contained in the first order products, as well as to the so called “RESTREND” approach (see for instance Wessels et al. 2012), which assume linearity or even proportionality (RUE) between rainfall and NPP, assumption-free relation indicators between rainfall and NPP trends were generated. Separate indicators were prepared for the relation between rainfall and vegetation year greenness, cyclic vegetation, and dry season greenness, respectively (see maps P53, P54, and P55). In addition, the same type of indicator was derived for a time span prior to the MERIS period (1981-2002), using GPCP rainfall data and NOAA GIMMS NDVI data (see map P56).

Table 2: Overview of the Indicator Maps shown in the booklets

Product number	Product name	Product description
1	Vegetation year average greenness 2003-2010	Vegetation year average greenness 2003-2010 26 greenness classes Mean of 8 vegetation years average values
2	Cyclic vegetation greenness 2003-2010	Cyclic vegetation greenness 2003-2010 26 greenness classes Mean of 8 cyclic fraction sum values
3	Dry season greenness 2003-2010	Dry season greenness 2003-2010 26 greenness classes Mean of 8 dry season average values
4	Variability of vegetation year greenness 2003-2010	Vegetation year greenness variability 2003-2010 26 greenness variability classes Variation coefficient of 8 vegetation year average values
8	Rain Use Efficiency of vegetation year average 2003-2010	Vegetation year RUE mean 2003-2010 26 RUE classes Mean of 8 vegetation year RUE values
17	Soil Moisture Use Efficiency of vegetation year average 2003-2010	Vegetation year SMUE 2003-2010 26 SMUE classes Mean of 8 vegetation year SMUE values
25	TRMM precipitation average of vegetation years 2003-2010	Vegetation year trmm rainfall mean 2003-2010 26 trmm rainfall classes Mean of 8 vegetation year rainfall sum values
26	TRMM precipitation variability of vegetation years 2003-2010	Vegetation year trmm rainfall variability 2003-2010 26 trmm rainfall variability classesVariation coefficient of 8 vegetation year rainfall sum values
29	Soil Moisture average of vegetation years 2003-2010	Vegetation year CCI Soil Moisture mean 2003-2010 26 SM classes Mean of 8 vegetation year SM average values
30	Soil Moisture variability of vegetation years 2003-2010	Vegetation year CCI Soil Moisture variability 2003-2010 26 SM variability classes Variation coefficient of 8 vegetation year SM average values
37	Rain Use Efficiency trend slopes of cyclic vegetation 2003-2010	Trendslope of cyclic fraction RUE 2003-2010 12 slope classes Theil-Sen median trend, masked at p 0.9
40	Soil Moisture Use Efficiency trend slopes of cyclic vegetation 2003-2010	Trendslope of cyclic fraction SMUE 2003-2010 12 slope classes Theil-Sen median trend, masked at p 0.9
46	Change in vegetation year precipitation between the epochs 2003-2006 and 2007-2010	Epochal difference of vegetation year TRMM rainfall 2003-2006 and 2007-2010 12 difference classes
50	Functional Classes	Relation between vegetation year greenness classes and the classified percentage of the cyclic vegetation of the yearly vegetation 2003-2010

51	Functional Differences	Epochal (2003-2006/2007-2010) diffrence map of the relation between vegetation year greenness classes and the classified percentage of the cyclic vegetation of the yearly vegetation
52	Seasonal Trend Relations	Relation between vegetation year greenness trends and seasonal greenness trends 2003-2010
53	TRMM Rainfall versus MERIS fAPAR vegetation year greenness trend	Relation between vegetation year rainfall trends and vegetation year greenness trends 2003-2010
54	TRMM Rainfall versus MERIS fAPAR cyclic fraction greenness trend	Relation between cyclic fraction rainfall trends and cyclic fraction greenness trends 2003-2010
55	TRMM Rainfall versus MERIS fAPAR dry season greenness trend	Relation between vegetation year rainfall trends and dry season greenness trends 2003-2010
56	GPCP Rainfall versus GIMMS NDVI vegetation year greenness trend	Relation between vegetation year GPCP rainfall trends and vegetation year greenness (GIMMS NDVI) trends 1981-2002
57	Median start of vegetation year 2003-2010	Median of the start times (half month number in the calendar year) of the vegetation year 2003-2010
58	Mean length of vegetation season 2003-2010	Mean of the lenghts of the vegetation seasons 2003-2010
59	Mean start time of vegetation season 2003-2010	Average start time (half month number in the calendar year) of the vegetation seasons 2003-2010

All map products shown in the booklet, and all other map products (which are of similar kind but with different seasonal and water parameter combinations) along with meta data, product lists and short descriptions can be downloaded at http://www.diversity2.info/products/ .

4.3 Selected Indicator Maps

In the next section, the listed indicator maps are shown with descriptions. First, the three phenological maps (P57 – P59) are displayed, followed by the second oder indicator maps (P50 – P56, with P46 included). The last three pages contain representative first order indicator status and trend maps (P1 – P40).

P57 Median start of vegetation year 2003-2010

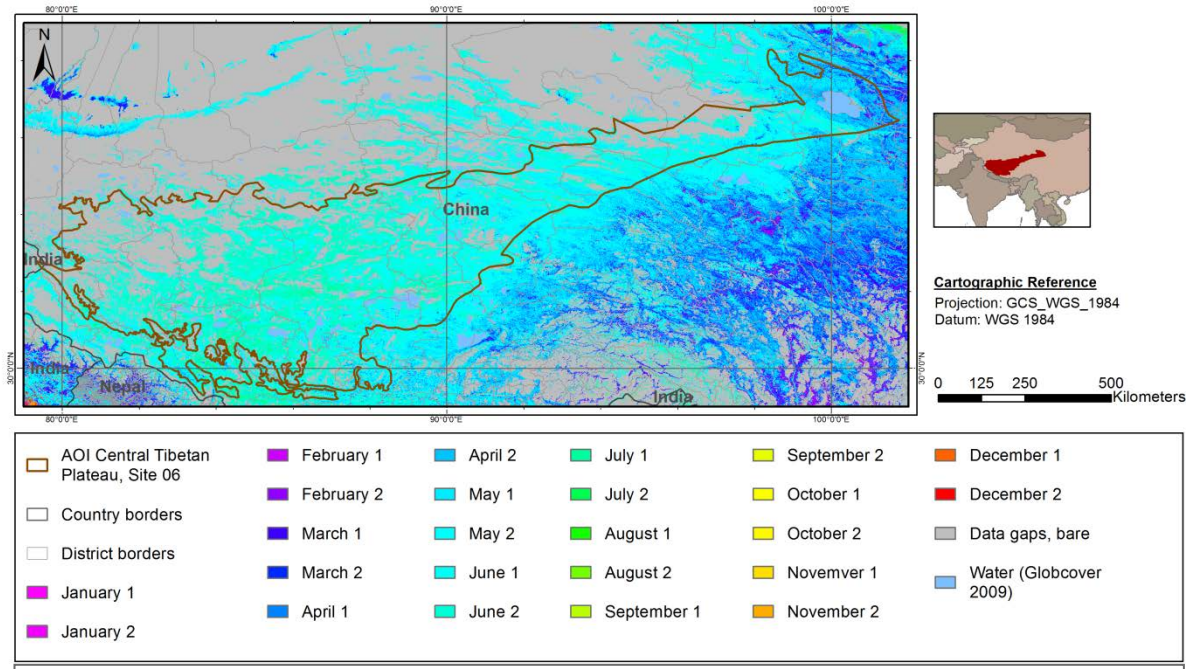

P57 Median start of vegetation year 2003-2010

The median value of the start of the vegetation year refers to the time when vegetation development is about to start, and is as such a very early indicator of the start of the vegetation season. The locally dominating start time, i.e. the most frequently occurring time period has been selected in cases where more than one start time (range) is being observed, considering their yearly fluctuations. This indicator shows the median value of the eight start times 2003-2010. The numbers behind the month names refer to the first and second half of each month, respectively.

P58 Mean length of vegetation season 2003-2010

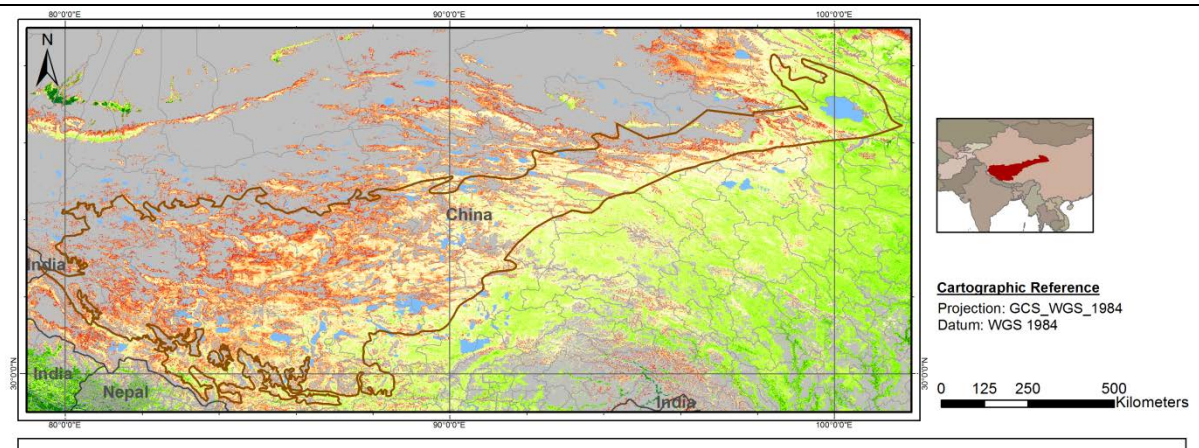

P58 Mean length of vegetation season 2003-2010

The mean length of the vegetation season (LOS) refers to the duration of the green peak(s) (cyclic fraction) of the vegetation within a vegetation year. It is negatively correlated with aridity, but by far not totally explained by the latter. The season, when the rain falls plays a role, and especially land cover/use, which determine largely the duration of the green period within given humidity ranges. In irrigated areas, LOS is +/-decoupled from climatic constraints.

P59 Mean start of vegetation season 2003-2010

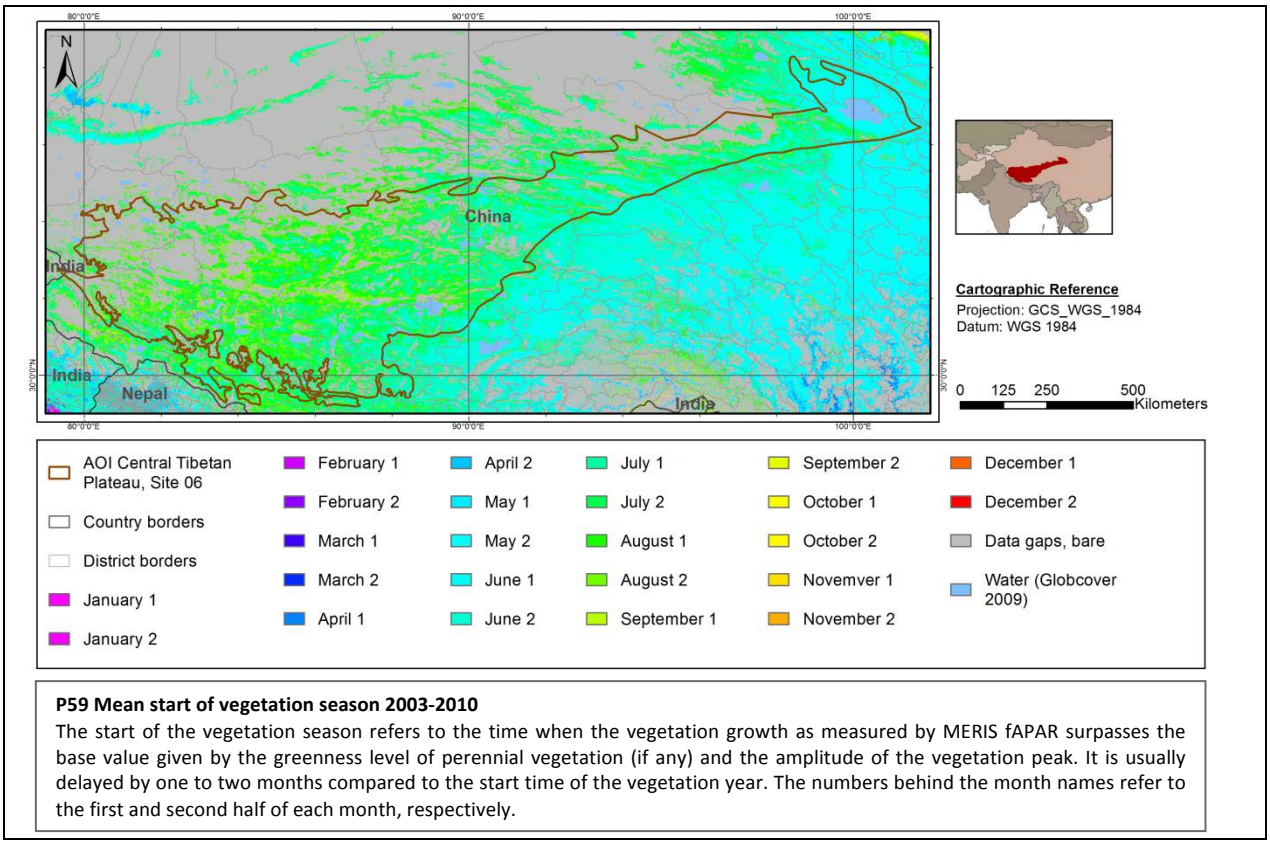

P59 Mean start of vegetation season 2003-2010

The start of the vegetation season refers to the time when the vegetation growth as measured by MERIS fAPAR surpasses the base value given by the greenness level of perennial vegetation (if any) and the amplitude of the vegetation peak. It is usually delayed by one to two months compared to the start time of the vegetation year. The numbers behind the month names refer to the first and second half of each month, respectively.

P50 Functional classes

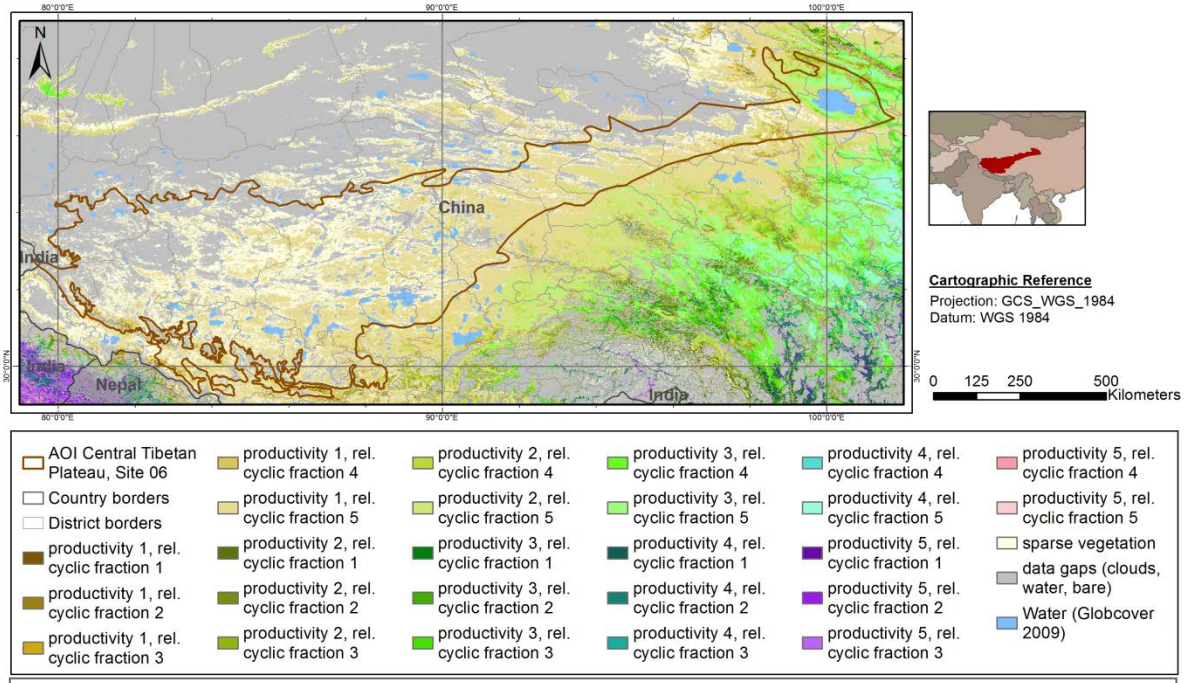

P50 Functional classes

The functional classes originate from a combined classification of vegetation productivity and the percentage of cyclic vegetation of the yearly vegetation. The numbers in the legend increase with increasing values of these parameters. The lighter the tone, the higher is the percentage of the cyclic vegetation and the lower probably the share of woody evergreen vegetation. The respective map is closely related to land use/cover patterns and to soil and terrain type and structures.

P52 Seasonal trend relations

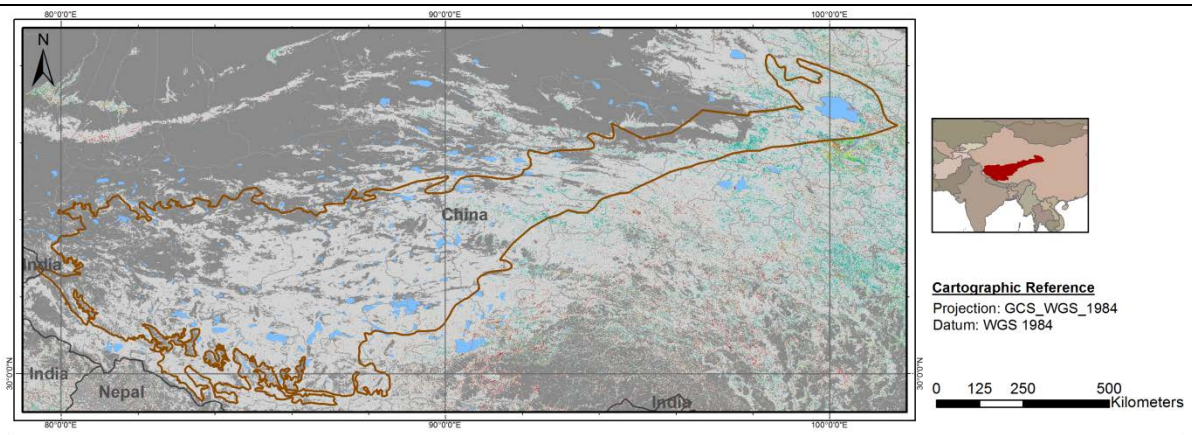

P52 Seasonal trend relations

The seasonal trend relation for the years 2003-2010 shows how vegetation year changes in productivity are partitioned into trends of the cyclic vegetation and/or trend of the dry season greenness. The brown and purple classes for instance show areas where the dry season vegetation has increased, whereas the cyclic vegetation shows negative or no trends. These areas may point to possible further growth of bushes/trees at the expense of annual vegetation.

P51 Functional differences

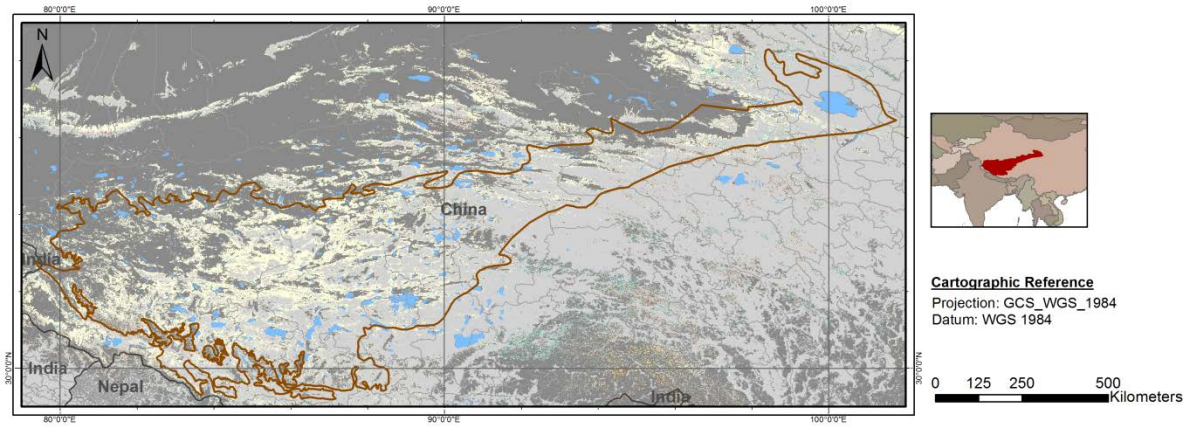

AOI Central Tibetan Plateau, Site 06	NPP increase	PC cycfrac no change	NPP decrease	PC cycfrac decrease	
Country borders	NPP no change	PC cycfrac increase	NPP decrease	PC cycfrac no change	
District borders	NPP no change	PC cycfrac decrease	Sparse vegetation		
NPP increase	PC cycfrac increase	NPP no change	PC cycfrac no change	Data gaps (clouds, water, bare)	
NPP increase	PC cycfrac decrease	NPP decrease	PC cycfrac increase	Water (Globcover 2009)	

P51 Functional differences
The functional differences are the epochal differences (2003-2006/2007-2010) between the indicator P50 calculated for these two epochs. The yellow class for instance shows areas with an increase of the vegetation year greenness, but with a largely stable percentage of the cyclic vegetation of the yearly vegetation productivity. Compared to P52, which is a trend product, P51 is a change product with rather strict thresholds.

P46 Change in vegetation year precipitation between epochs 2003-2006 and 2007-2010

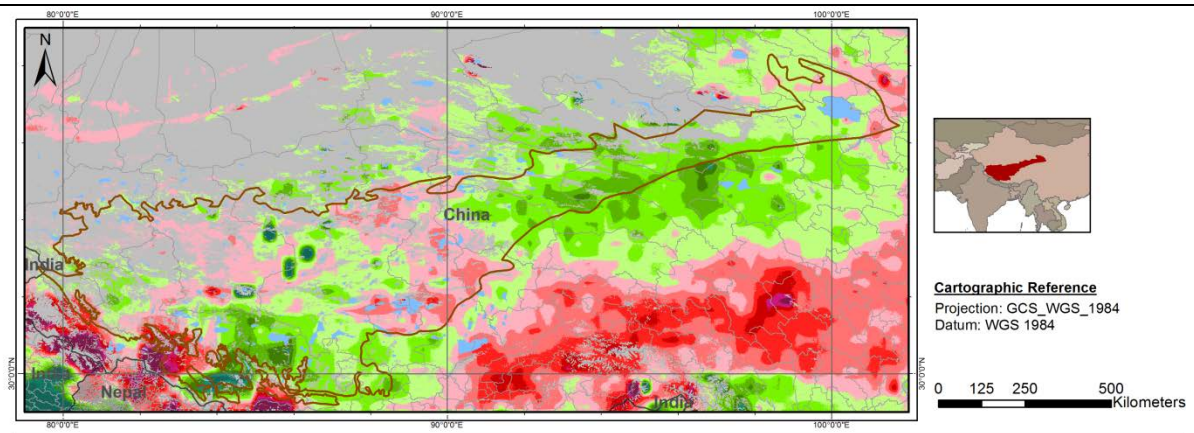

AOI Central Tibetan Plateau, Site 06	yearly decrease	120 - 160	yearly increase	40 - 80	Data gaps/no rainfall		
Country borders	yearly decrease	80 - 120	yearly increase	80 - 120	Water (Globcover 2009)		
District borders	yearly decrease	40 - 80	yearly increase	120 - 160			
yearly decrease	> 200	yearly decrease	0 - 40	yearly increase	160 - 200		
yearly decrease	160 - 200	yearly increase	0 - 40	yearly increase	> 200		

P46 Change in vegetation year precipitation between epochs 2003-2006 and 2007-2010
Change in TRMM 3b42 precipitation between the two epochs 2003-2006 and 2007-2010. Per epoch, the rainfall has been averaged over the four vegetation years. The epochal change is given by the difference between the yearly average precipitation of the two epochs in mm.

P56 GPCP rainfall versus GIMMS NDVI vegetation year greenness trends 1981-2002

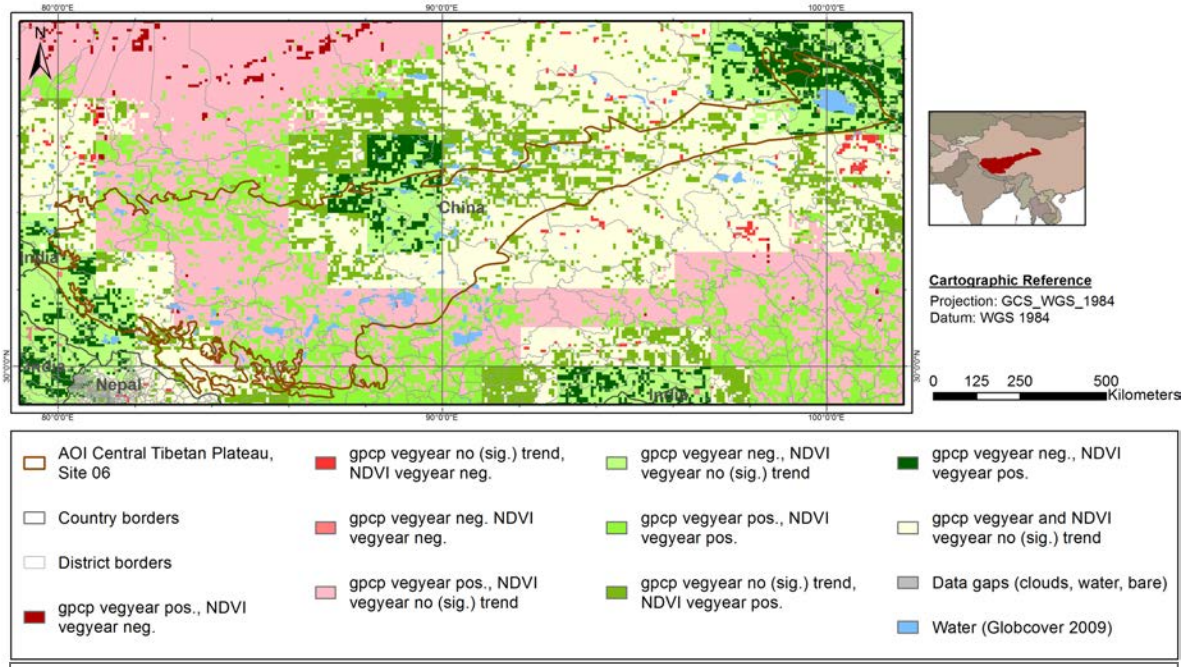

P56 GPCP rainfall versus GIMMS NDVI vegetation year greenness trends
This indicator shows the NOAA GIMMS based vegetation trends for the vegetation years 1981-2002 in relation to the GPCP rainfall trends. This product combines all trends and thus highlights regions with rainfall and vegetation trends of equal direction and those of opposite directions. The light pink areas e.g. exhibit positive GPCP rainfall trends, which are not matched by positive NDVI trends.

P54 TRMM rainfall versus MERIS fAPAR cyclic fraction greenness trends 2003-2010

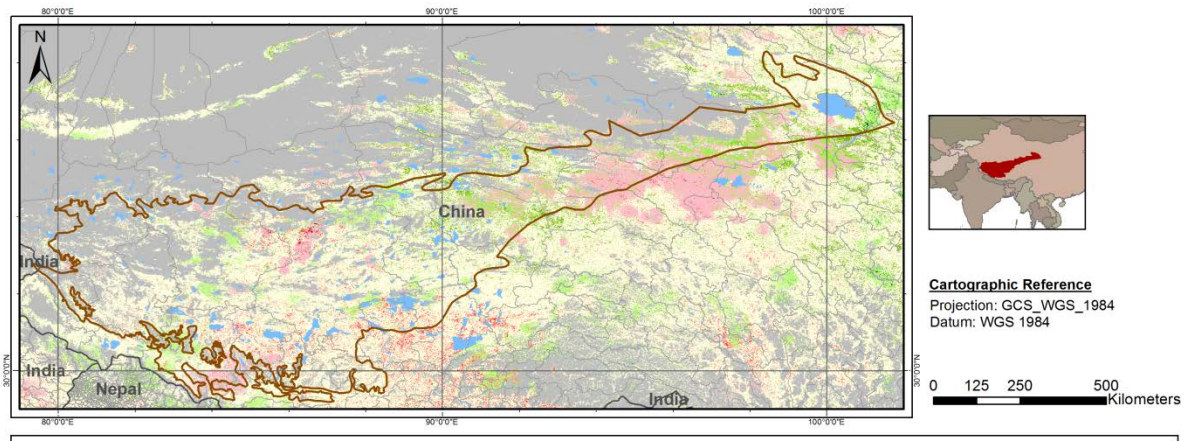

P54 TRMM rainfall versus MERIS fAPAR cyclic fraction greenness trends 2003-2010
This indicator shows the MERIS fAPAR based cyclic vegetation trends for the vegetation years 2003-2010 in relation to the TRMM rainfall trends. This indicator combines all trends and thus highlights regions with rainfall and vegetation trends of equal direction and those of opposite directions. The light pink areas e.g. exhibit positive TRMM rainfall trends, which are not matched by positive fAPAR trends.

P53 TRMM rainfall versus MERIS fAPAR vegetation year greenness trends 2003-2010

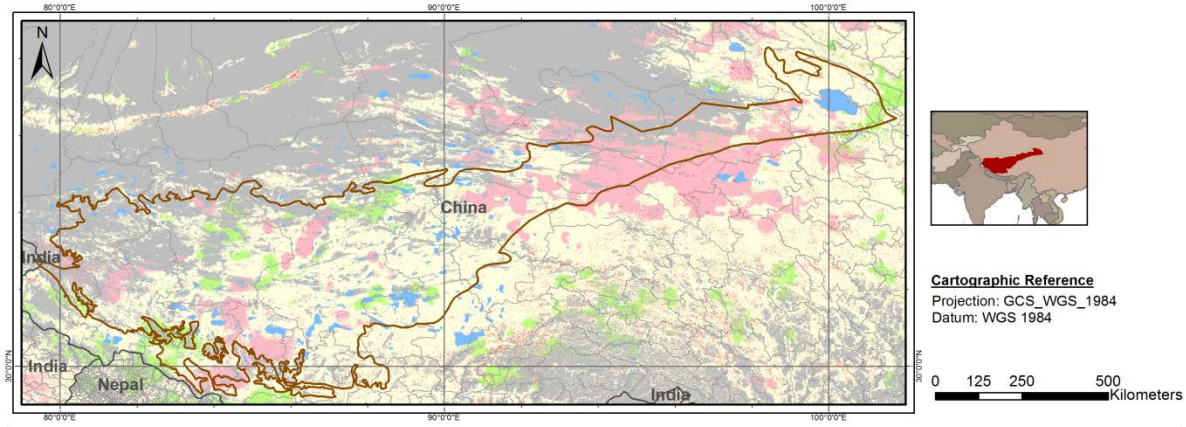

AOI Central Tibetan Plateau, Site 06
Country borders
District borders
trmm vegyear pos., fapar vegyear neg.
trmm vegyear no (sig.) trend, fapar vegyear neg.
trmm vegyear neg. fapar vegyear neg.
trmm vegyear pos., fapar vegyear no (sig.) trend
trmm vegyear neg., fapar vegyear no (sig.) trend
trmm vegyear pos., fapar vegyear pos.
trmm vegyear no (sig.) trend, fapar vegyear pos.
trmm vegyear neg., fapar vegyear pos.
trmm vegyear and fapar vegyear no (sig.) trend
Data gaps (clouds, water, bare)
Water (Globcover 2009)

P53 TRMM rainfall versus MERIS fAPAR vegetation year greenness trends 2003-2010

This indicator shows the MERIS fAPAR based vegetation year greenness trends for the vegetation years 2003-2010 in relation to the TRMM rainfall trends. This indicator combines all trends and thus highlights regions with rainfall and vegetation trends of equal direction and those of opposite directions. The light green areas e.g. exhibit negative TRMM rainfall trends, which are not matched by negative fAPAR trends.

P55 TRMM rainfall versus MERIS fAPAR dry season greenness trends 2003-2010

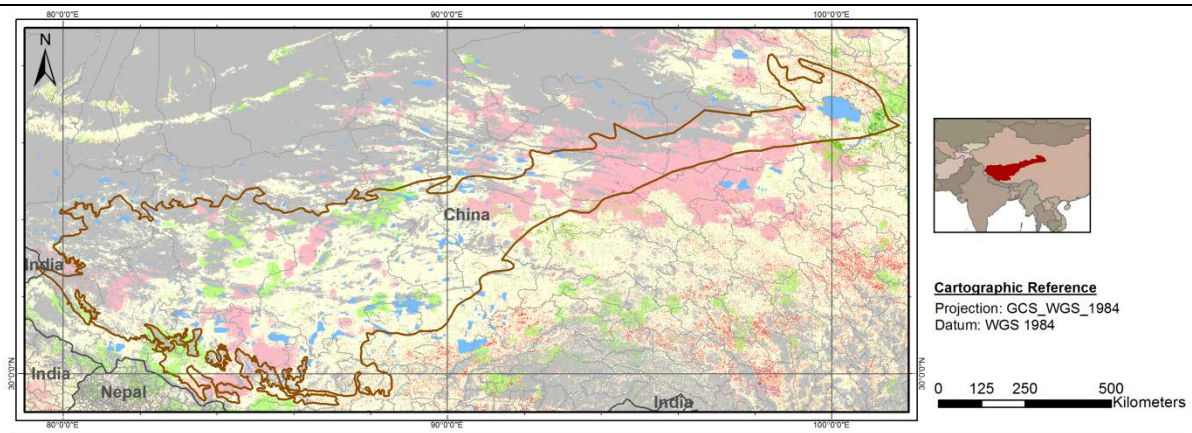

AOI Central Tibetan Plateau, Site 06
Country borders
District borders
trmm vegyear pos., fapar dry season neg.
trmm vegyear no (sig.) trend, fapar dry season neg.
trmm vegyear neg. fapar dry season neg.
trmm vegyear pos., fapar dry season no (sig.) trend
trmm vegyear neg., fapar dry season no (sig.) trend
trmm vegyear pos., fapar dry season pos.
trmm vegyear no (sig.) trend, fapar dry season pos.
trmm vegyear neg., fapar dry season pos.
trmm vegyear and fapar dry season no (sig.) trend
Data gaps (clouds, water, bare)
Water (Globcover 2009)

P55 TRMM rainfall versus MERIS fAPAR dry season greenness trends 2003-2010

This indicator shows the MERIS fAPAR based dry season vegetation trends for the vegetation years 2003-2010 in relation to the TRMM rainfall trends. This indicator combines all trends and thus highlights regions with rainfall and vegetation trends of equal direction and those of opposite directions. The light red areas e.g. exhibit areas without TRMM rainfall trends that show negative dry season fAPAR trends.

P01 Vegetation year average greenness 2003-2010

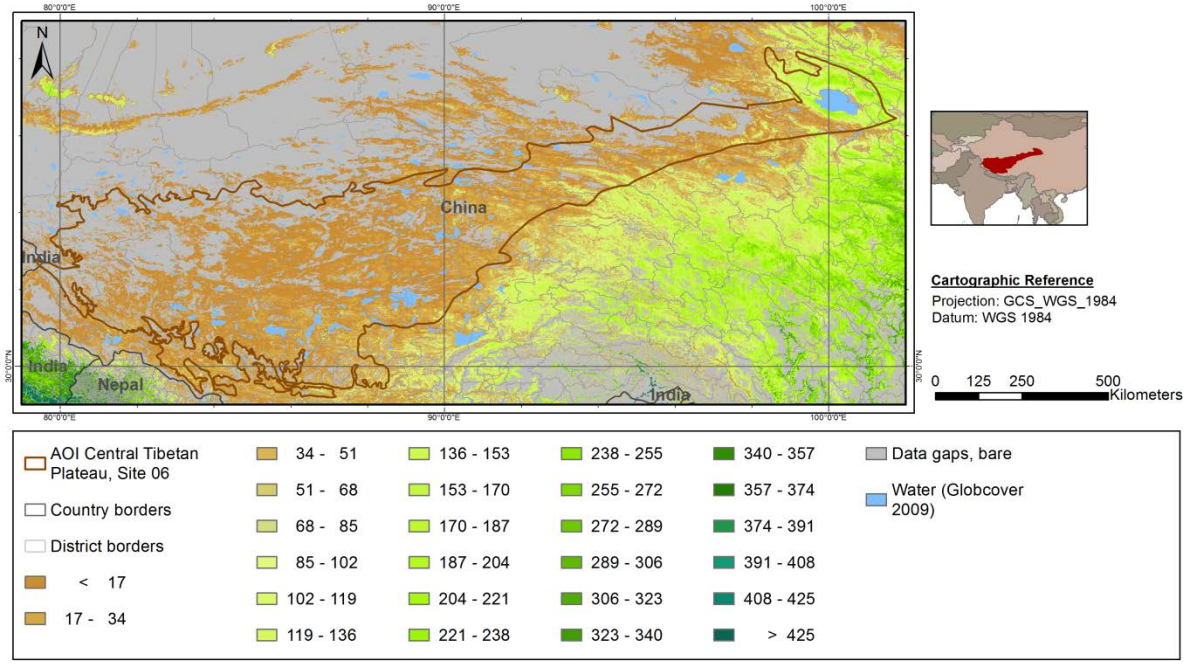

P01 Vegetation year average greenness 2003-2010
Status of MERIS fAPAR average vegetation year greenness, calculated as mean value of the vegetation years 2003-2010. Brownish tones correspond to extremely dry conditions, grading into light and then dark green to dark bluish green tones in humid regions or locations with dense vegetation. The original fAPAR values [0-1] have been multiplied with 1000.

P04 Variability of vegetation year greenness 2003-2010

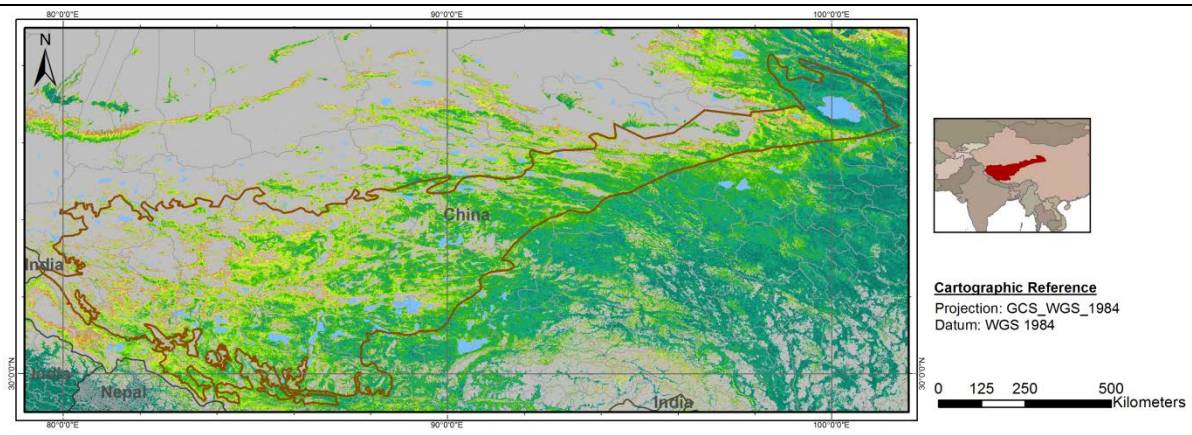

P04 Variability of vegetation year greenness 2003-2010
Variability of MERIS fAPAR vegetation year greenness is expressed by the coefficient of variation of the vegetation years 2003-2010. As the variability in general increases with increasing dryness, the reverse colours were given to the classes in relation to the average classes. Especially interesting may be areas which do not follow the general pattern of reversal compared to the average greenness values.

P02 Cyclic vegetation greenness 2003-2010

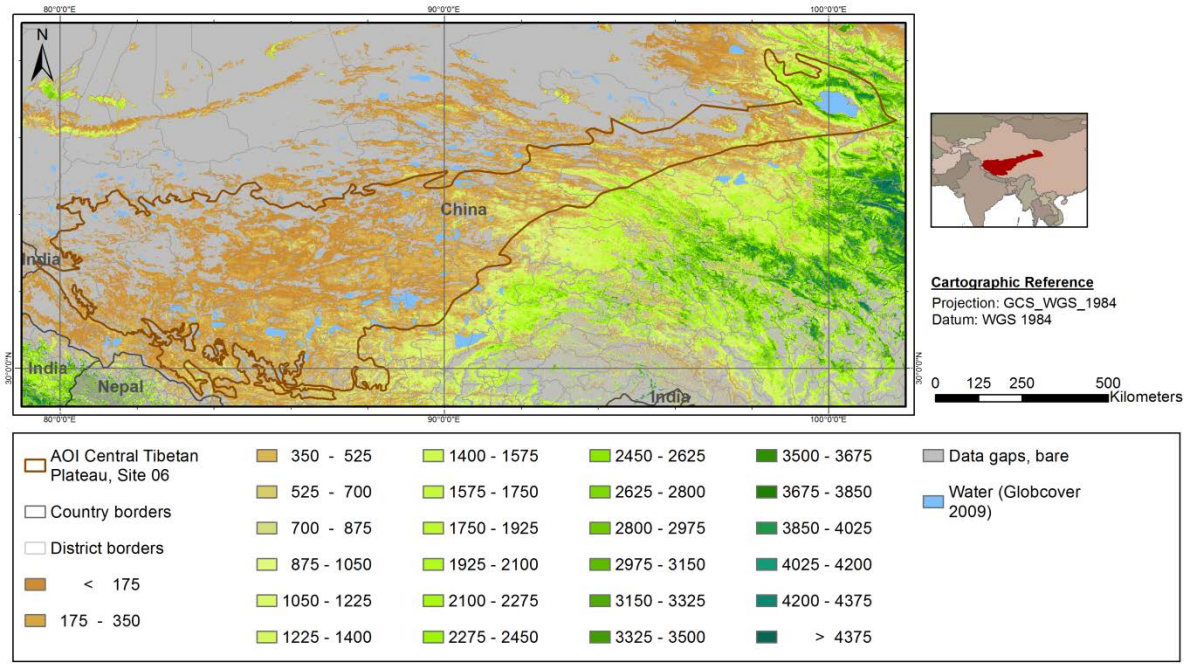

P02 Cyclic vegetation greenness 2003-2010
Status of MERIS fAPAR cyclic vegetation greenness calculated as mean value for the vegetation years 2003-2010. The cyclic fraction of the vegetation is comprised of summed fAPAR values of the green peak(s) during a vegetation year, subtracting the non-cyclic base levels. The original fAPAR values [0-1] have been multiplied with 1000.

P03 Dry season greenness 2003-2010

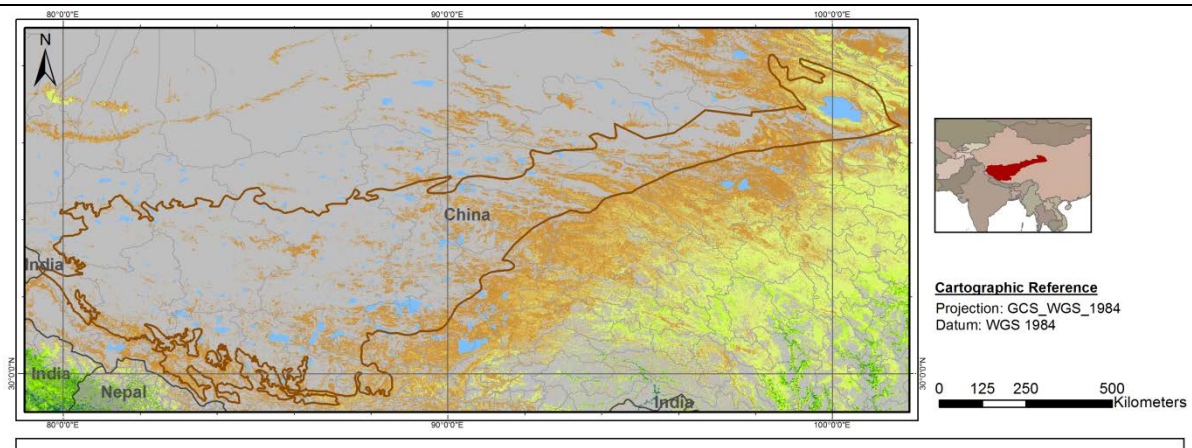

P03 Dry season greenness 2003-2010
Status of MERIS fAPAR dry season greenness calculated as mean value for the period 2002-2011. The dry season values reflect the portion of plants that remain green after senescence of the annual vegetation or grow new green leaves during the dry period. The original fAPAR values [0-1] have been multiplied with 1000.

P08 Rain Use Efficiency of vegetation year average 2003-2010

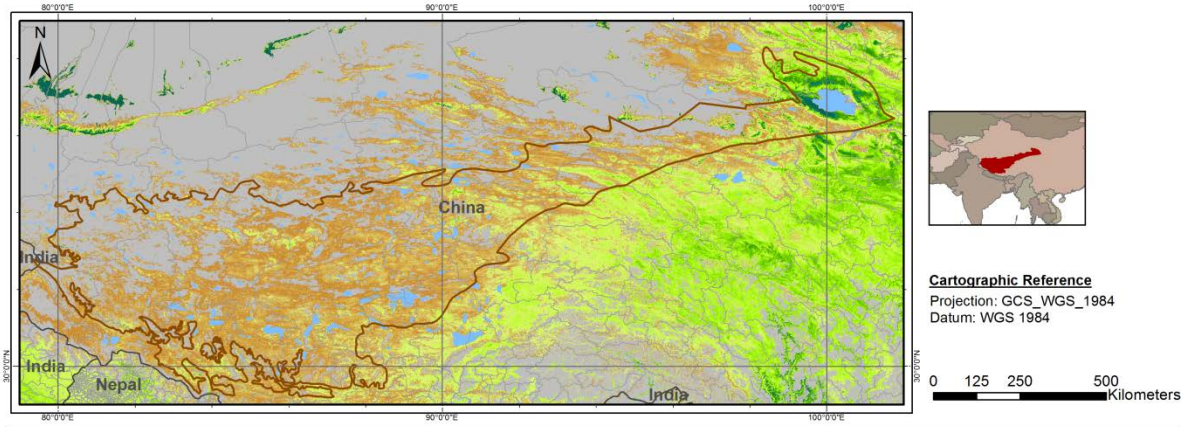

P08 Rain Use Efficiency of vegetation year average 2003-2010
Status of the Rain Use Efficiency based on the MERIS fAPAR vegetation year greenness of 2003-2010 and TRMM 3b42 rainfall data. It is calculated by dividing the average fAPAR values (of the vegetation years) by the average rainfall of the vegetation years. The TRMM data are resampled to technically match the MERIS fAPAR spatial resolution, knowing that their actual spatial resolution of 0.25° does not (!) match the MERIS fAPAR data of 300m. RUE is considered to indicate how efficiently rain water is utilised for vegetation growth.

P17 Soil Moisture Use Efficiency of vegetation year average 2003-2010

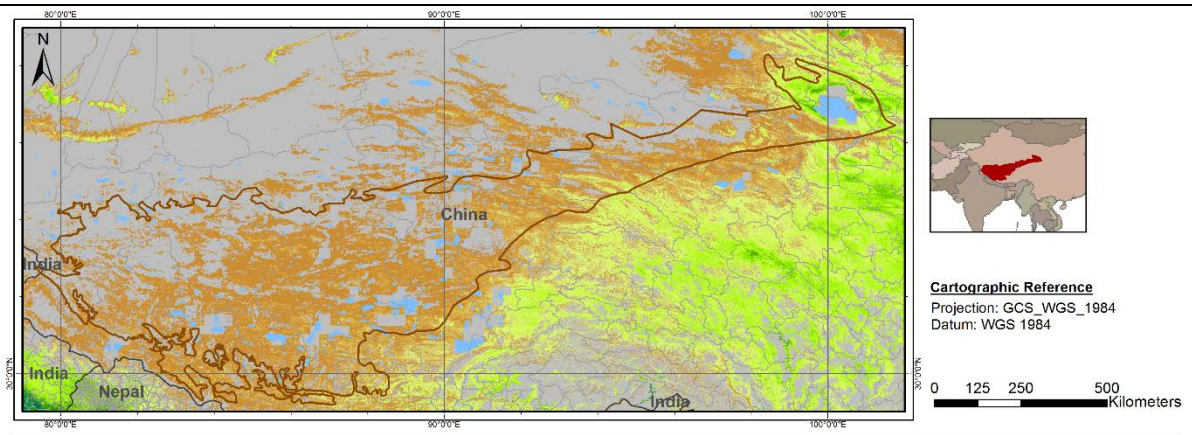

P17 Soil Moisture Use Efficiency of vegetation year average 2003-2010
Status of the Soil Moisture Use Efficiency based on the MERIS fAPAR vegetation year greenness of 2003-2010 and CCI soil moisture data. It is calculated by dividing the average fAPAR values (of the vegetation years) by the average soil moisture of the vegetation years. The SM data are resampled to technically match the MERIS fAPAR spatial resolution, knowing that their actual spatial resolution of 0.25° does not (!) match the MERIS fAPAR data of 300m. SMUE is considered to indicate how efficiently soil moisture is utilised for vegetation growth. The original SM values reach from 0 to 1 and have been stretched from 0 to 1000.

P37 Rain Use Efficiency trend slopes of cyclic vegetation 2003-2010

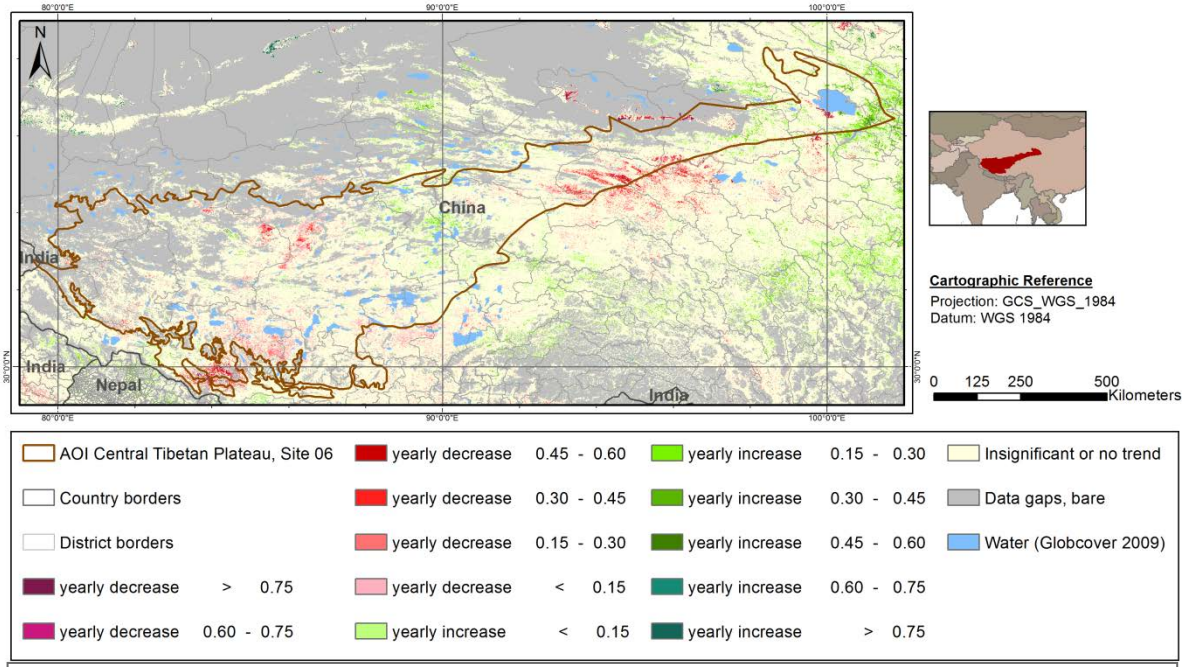

P37 Rain Use Efficiency trend slopes of cyclic vegetation 2003-2010
Trend slopes of cyclic fraction Rain Use Efficiency values for the period 2002-2011, based on MERIS fAPAR data and TRMM 3b42 rainfall data. RUE is calculated by dividing the cyclic fraction sums of the vegetation by the corresponding integrated rainfall data. RUE is considered to indicate how efficiently rain water is utilised for vegetation growth. Trends are calculated using the median trend estimator of Theil (1950) and Sen (1968) and the significance test (p 0.1) of Mann (1945) and Kendall (1975). Trend values indicate average change per year. The original fAPAR values reach from 0 to 1 and have been stretched from 0 to 1000.

P40 Soil Moisture Use Efficiency trend slopes of cyclic vegetation 2003-2010

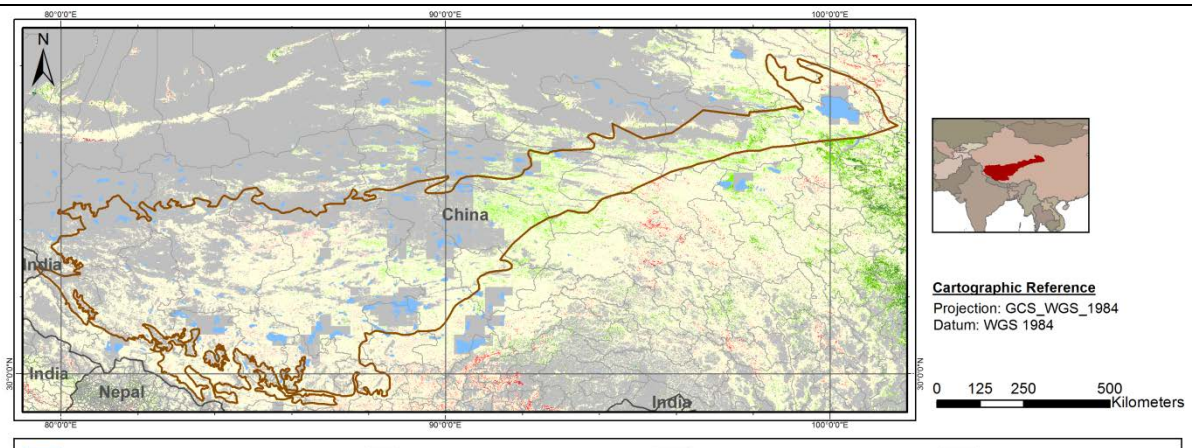

P40 Soil Moisture Use Efficiency trend slopes of cyclic vegetation 2003-2010
Trend slopes of cyclic fraction Soil Moisture Use Efficiency values for the period 2002-2011, based on MERIS fAPAR data and CCI soil moisture data. SMUE is calculated by dividing the cyclic fraction sums of the vegetation by the corresponding integrated SM data. SMUE is considered to indicate how efficiently soil moisture is utilised for vegetation growth. Trends are calculated using the median trend estimator of Theil (1950) and Sen (1968) and the significance test (p 0.1) of Mann (1945) and Kendall (1975). Trend values indicate average change per year. The original fAPAR and SM values, respectively, reach from 0 to 1 and have been stretched from 0 to 1000.

P25 TRMM precipitation average of vegetation years 2003-2010

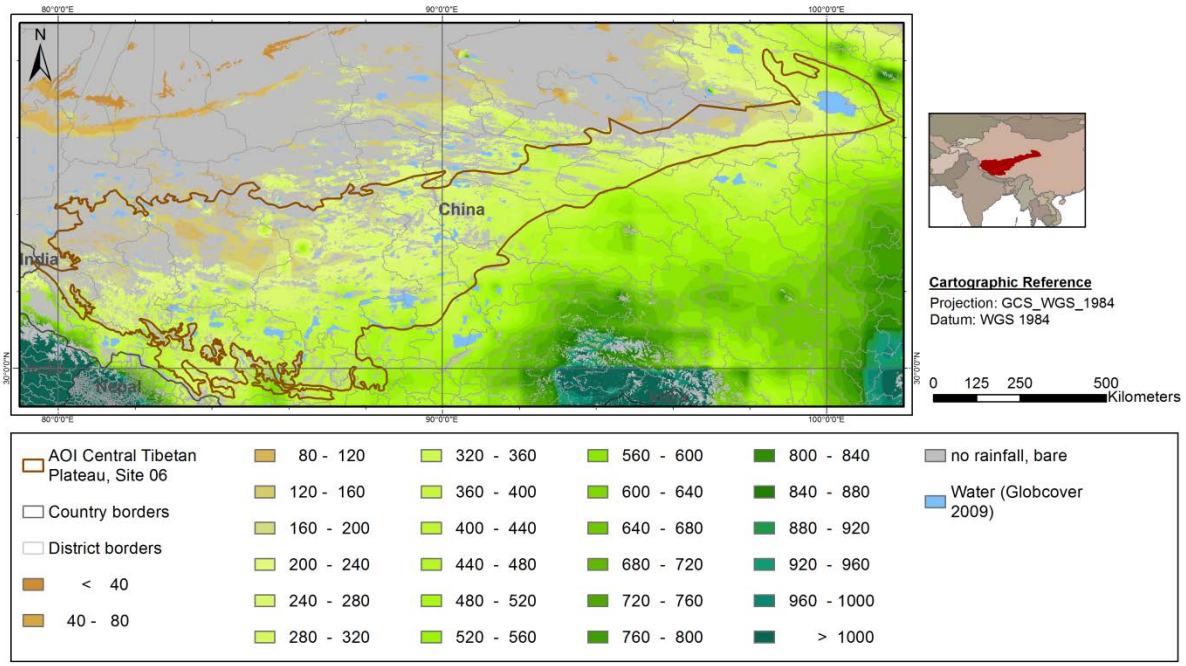

P25 TRMM precipitation average of vegetation years 2003-2010
Rainfall status derived from TRMM 3b42 rainfall data integrated over vegetation years and calculated as average rainfall sum values for the vegetation years 2003-2010 in mm.

P26 TRMM precipitation variability of vegetation years 2003-2010

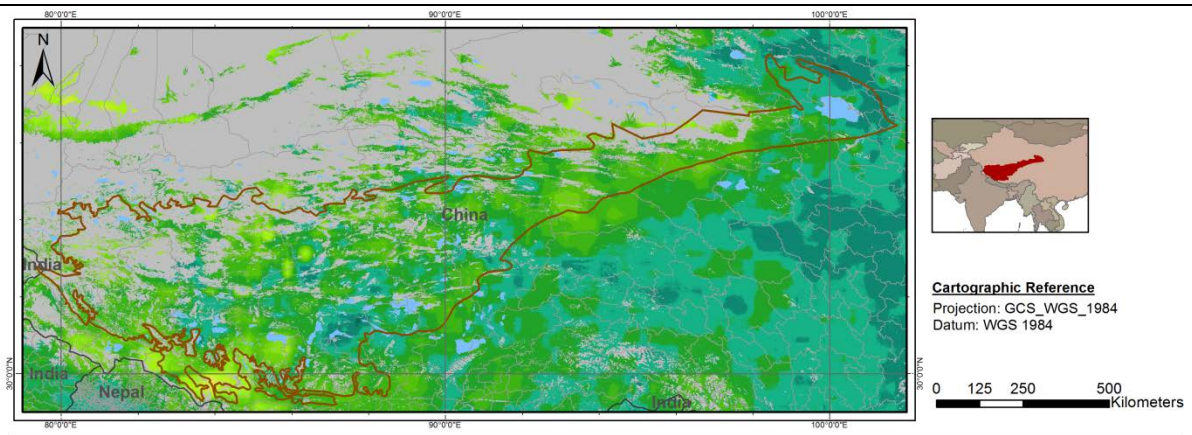

P26 TRMM precipitation variability of vegetation years 2003-2010
Rainfall variability derived from TRMM 3b42 rainfall data integrated over vegetation years and calculated as coefficient of variation of the vegetation year rainfall sums 2003-2010.

P29 Soil Moisture average of vegetation years 2003-2010

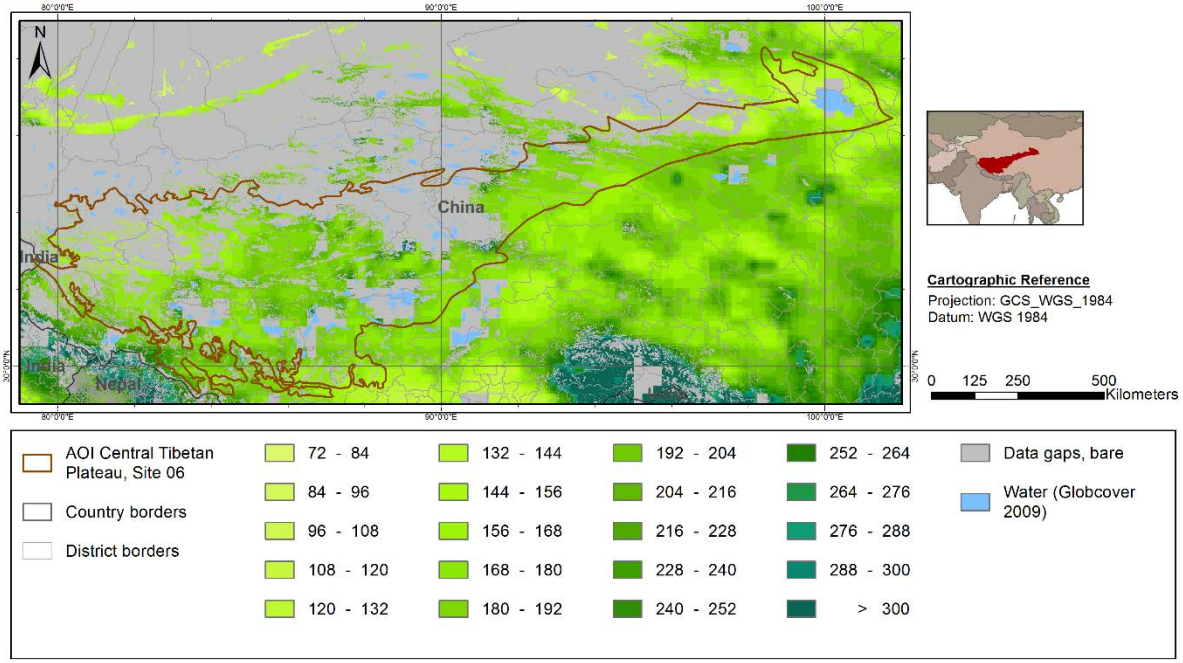

P29 Soil Moisture average of vegetation years 2003-2010
Soil moisture status derived from CCI soil moisture data integrated over vegetation years and calculated as mean soil moisture average values for the vegetation years 2003-2010.

P30 Soil Moisture variability of vegetation years 2003-2010

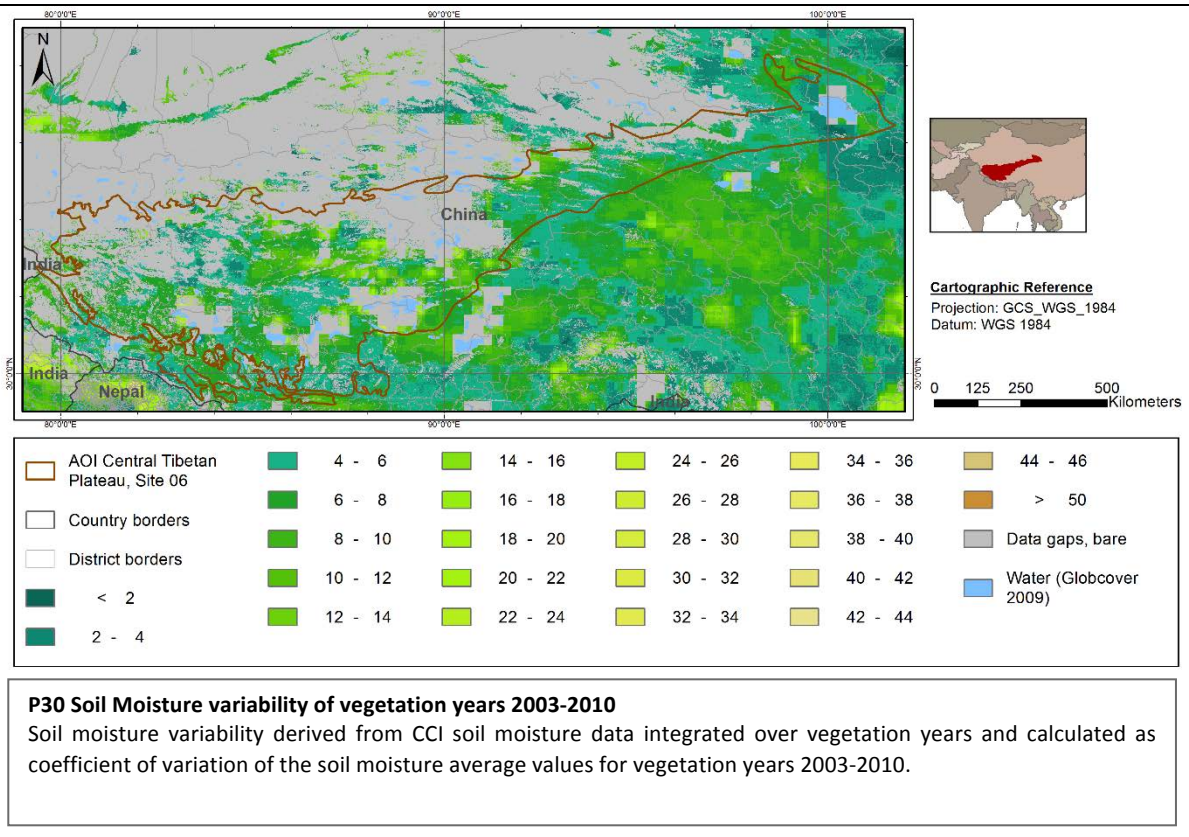

P30 Soil Moisture variability of vegetation years 2003-2010
Soil moisture variability derived from CCI soil moisture data integrated over vegetation years and calculated as coefficient of variation of the soil moisture average values for vegetation years 2003-2010.

5 Generic Interpretation of the Maps

While vegetation productivity obvious follows the rainfall gradients at the large scale (not considering temperature and radiation differences), the smaller scale differentiations exhibit the presence of further influences on vegetation growth at more local scales. These local and regional factors are especially land use, soil properties, topography, and hydrology and include also the protection status of areas. For instance many linear features with (mostly) higher NPP proxy and RUE values than their surroundings can be related to river valleys (often with only seasonal or ephemeral surface water).

Biomes with rich floristic biodiversity may be expected to exhibit higher NPP response to rainfall throughout the year as diverse plant communities may be characterised by a high phenological variability with optimised water exploitation. An example with an extended area of extraordinary high average RUE conditions is the Succulent Karoo biome in South Africa ("*The Succulent Karoo is notable for the world's richest flora of succulent plants, and harbours about one-third of the world's approximately 10,000 succulent species*" http://en.wikipedia.org/wiki/Succulent_Karoo). The same area is also characterised by an extended length of the green season (compared to areas with similar yearly rainfall), and a winter rain regime. Thus, phenological maps reveal important ecosystem conditions and gradients.

The differentiation of the NPP and RUE indicators into phenological periods helps diagnose the seasonal behaviour of the vegetation and thus provides clues about the presence and dominance of evergreen perennial vegetation versus annual vegetation (e.g. annual grasses, most crops). Accordingly, changes and trends of the phenological vegetation behaviour can be used as indicators for developments such as land use change and land cover change. For instance the worldwide observed phenomenon of bush encroachment (woody encroachment, woody thickening) in drylands (Ratajczak et al. 2011) will lead to a shift of vegetation phenology, where especially an increase of dry season greenness, possibly, but not necessarily combined with a decrease of the cyclic greenness can be expected.

Bush encroachment in range lands is largely perceived as negative development, where the bushes lead to range land degradation by reducing grass cover and impeding the access of cattle to the remaining grass. Also impoverishment of biodiversity was frequently found as an effect of bush encroachment (Ratajczak et al. 2011). The greening trends especially in the dry season are indeed a widespread phenomenon in the derived NPP proxy maps, possibly pointing to continued bush encroachment or enhanced growth and greening of existing bushes, partly related to rainfall increases. Pronounced dry season greening may also be caused by the plantation of (especially evergreen) woody plants and forests. In case of greening trends related to commercial forest plantations, the trends can also be interpreted as a biodiversity loss.

Several indicators for the "classical" land degradation, i.e. the decrease of vegetation productivity in relation to available water have been derived in Diversity II. They include RUE and SMUE, where the latter is based on soil moisture, which is more directly reflecting available water in the root zone than rainfall. Often, RUE and SMUE exhibit different results, which is the logical consequence of the differences between the rainfall and the soil moisture data used. However, negative RUE trends are widely disputed as indicator for land degradation, mainly because RUE has been found to not consistently normalise for rainfall variability. Also the alternative RESTREND method has been challenged for this purpose (e.g. Wessels et al. 2012, Ratzmann 2014). In addition to their weaknesses related to invalid assumptions, they are lumped indicators, which do not detangle the individual developments of water availability and vegetation production. The proposed second order indicators, on the other hand (see maps P53 to P56), show both rainfall (or alternatively soil moisture) trends and NPP trends separately and synoptically.

RUE or SMUE changes and trends may be as well related to land cover/use/management changes, such as the conversion of rangeland into cropland, deforestation, etc. Especially processes such as

urbanisation or mining will lead to extreme NPP proxy and RUE decreases. Phenology helps to detangle some of the trends: for instance the clearing of shrubs, bushes and trees (e.g. for the conversion of rangeland into crop land) can be expected to lead especially to dry season NPP and RUE decreases. On the other hand, the frequently found greening trends in the dry season, at first glance positive trends, may even be primarily related to adverse processes such as bush encroachment. However, caution is also necessary in this respect, as also range land improvement and tree planting activities may lead to positive NPP and RUE or SMUE trends.

The derived indicators should not be directly interpreted in terms of land condition, degradation or respectively land improvement. They provide useful base information, especially when combined, but there is no single "all in one" indicator about land condition and trends. In situ knowledge about biophysical and socio-economic factors and systems (including past and present land tenure and land use practices, history of land degradation, population pressure, current policies and economic developments, etc.) is indispensable for an appropriate assessment of status, trends, and possible future developments.

Finally, the observation period is rather short, which basically hampers conclusions from derived trends. The variability of rainfalls and subsequently vegetation greenness from year to year is so significant in drylands that it certainly hides trends, which in such a short period may be rare and not very pronounced. Trends must pass certain statistical significance threshold (which has been set to 0.9 and thus relatively low in this project) to be recognised as significant trends. There may be more relevant and persistent changes going on than the trend maps for such a short period can show, and abrupt change events cannot be expected to exhibit gradual indicator developments and measurable trends. The rainfall trend maps for instance show hardly any significant trends, while the rainfall change map between the two epochs shows large positive and negative change regions with partly big epochal rainfall differences. Vice versa, due to the short observation period, measured significant trends may not really be part of persistent, longer term development but may already be reversed in the next epoch.

The meteorological and other environmental data used play also a significant role especially for the generation of the RUE and SMUE indicators. Compared to the MERIS data with 300m ground resolution, these datasets are extremely coarse and especially with regard to the soil moisture data by far not representative for the scale of local variability at the MERIS resolution.

For these reasons the eight vegetation years covered worldwide by MERIS are perhaps better suited for an overall assessment of the ecosystem structures and conditions, where the phenological characterisation of vegetation trends may provide hints about ecosystem functions and biodiversity. While many of the variations in vegetation production and productivity in drylands are short and medium term responses to varying water availability, the seasonal type of these responses may be taken as valuable information towards this aim.

6 Outlook

The provided indicators and – if requested – the underlying continuous data can be utilised to many more analyses than those performed in the Diversity II project. Interested users may contact us for further information what else besides the project downloads has been produced in the project, or which further possibilities may exist to deepen or extend the studies.

The applied methods for the extraction of phenological and vegetation productivity parameters can be used for other sensors, such as the upcoming Sentinel 2 and especially Sentinel 3 of the ESA Copernicus program, which will be the successor of the ENVISAT MERIS data. Also SPOT Vegetation, MODIS, or Proba-V data can serve to extend the analyses of this study by applying at least the same methodology, if the data are certainly not fully comparable. Bridging the data gap between MERIS and Sentinel 3 with its first planned launch in 2015 may be achieved this way.

References

Gobron N. (1999), Envisat's Medium Resolution Imaging Spectrometer (MERIS) Algorithm Theoretical Basis Document: FAPAR and Rectifed Channels over Terrestrial Surfaces. JRC Scientific and Technical Reports.

Le Houérou, H.N. (1984), Rain use efficiency: a unifying concept in arid-land ecology. Journal of Arid Environments, 7, 213-247.

Fensholt, R., Rasmussen, K., Kaspersen, P., Huber, S., Horion, S., Swinnen, E. (2013), Assessing Land Degradation/Recovery in the African Sahel from Long-Term Earth Observation Based Primary Productivity and Precipitation Relationships. Remote Sensing, 5, 664-686.

Kendall, M.G. (1962), Rank Correlation Methods, Charles Griffin and Company, London.

Mann, H.B. (1945), Non-parametric tests against trend. Econometrica, 13, 163-171.

Ratajczak, Z., Nippert, J.B. and Scott, L. (2011), The effects of woody encroachment on plant diversity in global grasslands and savannas: a meta-analysis. http://media.wix.com/ugd/d270f9_013ee3e8ed68377da3047468fb523488.pdf.

Ratzmann, G., (2014), EO-based Relationships BetweenVegetation and Rainfall in Drylands. Towards better understanding of eco-hydrological patterns and dynamics. Master's thesis at the Faculty of Science, University of Copenhagen.

Sen, P. K. (1968), Estimates of regression coefficients based on Kendall's tau. *J. Amer. Statist. Assoc.* 63, 1379–1389.

Theil, H. (1950), A rank-invariant method of linear and polynomial regression analysis I, II and III, Nederl. Akad. Wetensch. Proc., 53, 386–392, 521–525, 1397–1412.

Wessels, K.J., Van den Bergh, F., Scholes, R.J. (2012), Limits to detectability of land degradation by trend analysis of vegetation index data. Remote Sensing of Environment, 125, 10–22.

All Drylands Booklets are available on **www.diversity2.info**

Publisher	ESA Diversity II project
Editor	Ute Gangkofner (GeoVille, Austria)
Cover Design	ESA - EOGB (Earth Observation Graphic Bureau)

ESA DIVERSITY II PROJECT TEAM

European Space Agency
Project requirement definition; user interface; EO data provision; project control

Brockmann Consult GmbH, Germany
Prime contractor; project management; algorithms for preprocessing including atmospheric correction over land and lakes; software and production

GeoVille Information Systems GmbH
Drylands requirements analysis; algorithms for drylands; software and production

Brockmann Geomatics AB, Sweden
Biodiversity and user interface; algorithms for water quality retrieval and lake indicators; website; web GIS; communication and outreach

Research Centre in Biodiversity and Genetic Resources CIBIO, Portugal
User requirements engineering; product validation; biodiversity assessment

Consultants
Rasmus Fensholt (Uni Copenhagen)
Kurt Günther (DLR)

Editing Author: Ute Gangkofner

diversity drylands